High Performance PZT Thick Film Actuators Using In-Plane Polarisation

Autors: D. Ernst, B. Bramlage, S. E. Gebhardt, A. J. Schönecker

Contact:

Dipl.-Ing. (FH) Dörthe Ernst
Fraunhofer Institute for Ceramic Technologies and Systems (IKTS)
Winterbergstraße 28, 01277 Dresden, Germany
+49 351 2553-7224
Doerthe.Ernst@ikts.fraunhofer.de

Dipl.-Phys. Bernhard Bramlage
Fraunhofer Institute for Ceramic Technologies and Systems (IKTS)
Winterbergstraße 28, 01277 Dresden, Germany
+49 351 2553-7938
Bernhard.Bramlage@ikts.fraunhofer.de

Dr.-Ing. Sylvia E. Gebhardt
Fraunhofer Institute for Ceramic Technologies and Systems (IKTS)
Winterbergstraße 28, 01277 Dresden, Germany
+49 351 2553-7694
Sylvia.Gebhardt@ikts.fraunhofer.de

Dr. rer. nat. Andreas J. Schönecker
Fraunhofer Institute for Ceramic Technologies and Systems (IKTS)
Winterbergstraße 28, 01277 Dresden, Germany
+49 351 2553-7508
Andreas.Schoenecker@ikts.fraunhofer.de

I. Keywords

PZT, thick film, screen-printing, piezoceramic, in-plane, interdigitated electrodes

II. Abstract

Piezoceramic thick films offer the possibility of integrated functional components in planar design. They can be applied as sensors, actuators, ultrasonic transducers, transformers and generators. Typically, piezoceramic thick films are excited through the film thickness. In contrast, in-plane mode of excitation will be beneficial especially for actuator applications. The use of interdigitated electrodes (IDE) enables in-plane excitation of piezoceramic thick films. Actuator performance of cantilever structures with through-thickness and in-plane polarised piezoceramic thick films are investigated. The performance of in-plane polarised cantilevers depends on the particular IDE spacing. Using finite element simulations of the E-field distribution, geometrical and design efficiencies are considered and compared to experimentally derived data.

III. Introduction

Ceramic multilayer technology has been proven to be a suitable base for constructing robust microsystems. Several printing, stacking and laminating steps of ceramic green tapes enable three-dimensional electronic packaging and provide for a great geometrical flexibility and a high level of integration. Piezoceramic thick films allow for increased functionality *e.g.* for sensor and actuator application means. At Fraunhofer IKTS lead zirconate titanate (PZT) thick films have been developed and studied extensively during the last 15 years.[1] They are implemented in numerous applications such as adaptive mirrors, ultrasonic transducers and force sensors.[2,3]

The typical layer set-up of piezoceramic thick film devices found in literature consists of a substrate and a piezoceramic layer sandwiched between two flat electrodes (Fig. 1a).[4,5,6,7,8] Additional insulation layers allow for crossing of conductor paths. During excitation, the electrical field extends through the thickness of the film. Because of the d_{31}-effect the piezoceramic film contracts in plane direction. A cantilever based on the mentioned layer set-up will bend in direction of the piezoceramic thick film (Fig. 1a). The majority of piezoelectric devices utilise the much stronger d_{33}-effect. For implementation in a cantilever set-up, interdigitated electrodes (IDE) are essential (Fig. 1b). Bending of such cantilevers will be in direction of the substrate.

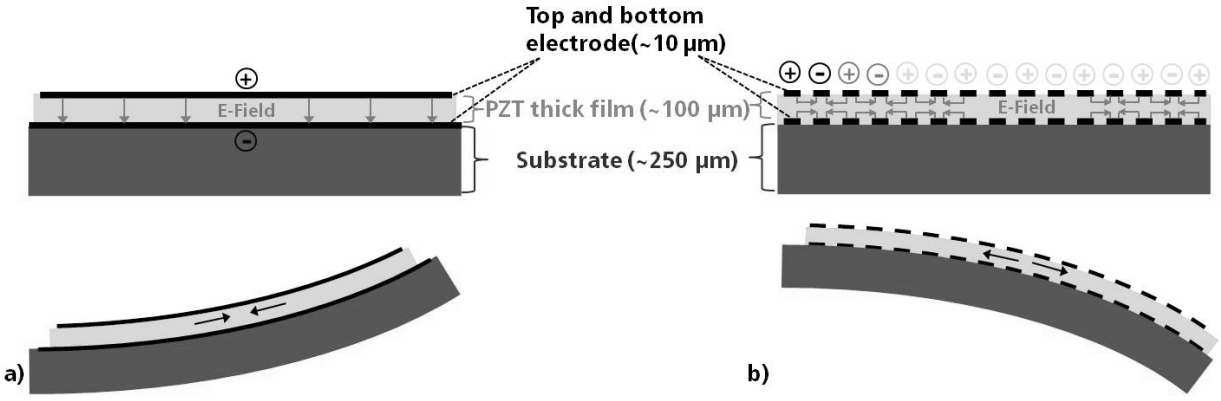

Fig. 1: Layer set-up with schematic E-field distribution and resulting bending behaviour during excitation of a) through-thickness polarized (d_{31}-effect) and b) in-plane polarized (d_{33}-effect) PZT thick film actuators

Interdigitated electrodes are well known from other piezoelectric devices, like Active Fiber Composites (AFC) or Macro Fiber Composites (MFC).[9,10] Xu et al. demonstrated this principle for PZT thin films.[11] Compared to through-thickness polarised films performance of in-plane polarised films will be doubled according to equation (1).

$$d_{33} \approx -2 \times d_{31} \tag{1}$$

Only few publications report on the use of IDEs for the excitation of PZT thick films. White et al. presented a surface acoustic wave sensor with screen printed Ag/Pd IDEs and a PZT covering layer on an alumina substrate.[12] De Cicco and Morten have published a principle study of PZT thick film trimorph actuators with in-plane polarisation using IDEs.[13]

The present work focuses on the experimental evaluation of large signal performance of cantilevers with in-plane polarised films in comparison to cantilevers with through-thickness polarised PZT films. The IDE design and the lateral actuator dimensions are described in detail in section IV and V. 2D finite element simulation (ANSYS) of the electrical field distribution is used to investigate and explain performance dependence on electrode distance as shown in paragraph VB.

IV. Experimental Methods

A. Sample Preparation

Unimorph cantilever beams were fabricated using screen-printing technology. The active structure was 4 mm in width and the length varied between 11 and 23 mm. The cantilevers were arranged as a comb structure and were processed in batches of 4 combs on one substrate. A bottom and top electrode (*e.g.* C5789, Heraeus) of ~15 µm, an intermediate piezoceramic thick film of ~100 µm and an insulating dielectric (QM 44 D, DuPont) of 40 µm thickness were screen-printed successively on a substrate. Films were sintered after each printing step. A 99.6 % alumina substrate (Rubalit® R710, Ceram Tec GmbH) was chosen because of low chemical interactions between the substrate material and the piezoceramic as recommended in literature.[14] Cantilever performance depends on thickness and young's modulus of the substrate as well as on thickness of PZT. Equation (2) was used to calculate the maximum of cantilever curvature c. d_{31} is the transverse piezoelectric charge constant, E is the electric field in the PZT layer, k is the ratio of the young's moduli $k = E_{substrate} / E_{PZT}$ and r is the ratio of the layer thickness $r = t_{substrate} / t_{PZT}$.

$$c = \frac{(d_{31}E)}{t_{PZT}} \times \frac{6kr(1+r)}{1+k^2r^4+2kr(2+3r+2r^2)} \tag{2}$$

For experiments a 270 µm thick Al_2O_3 substrate was used. In the calculations a young's modulus of 350 GPa was assumed for alumina. The young's modulus of the PZT thick film was measured by vickers hardness test and has a value of 80 GPa. The maximum of cantilever curvature c was calculated for a PZT thickness of 270 µm. Screen printing technology is not suitable for such thick films. If the layout additionally provides for electrode paths over high topographies processing becomes more difficult with increasing height difference and decreasing structure size. Therefore a PZT thickness of 100 µm was chosen. PZT thick film paste PZ 5100, developed at Fraunhofer IKTS was used for the experiments. It is based on a PZT powder (Sonox® P51, Ceram Tec GmbH) modified with low sintering additives.[15] Detailed investigations on PZ 5100 and the influence of the sintering aid content on electromechanical properties of PZ 5100 were

published elsewhere.[16] Sintering at 900 °C / 2 h produced a dense microstructure as depicted in Fig. 2. Insulating dielectrics were used to avoid short circuits at electrode crossings and/or to increase break down voltage between different electrical potentials. After fabrication, comb structures were separated from the substrate by laser machining as shown in Fig. 3.

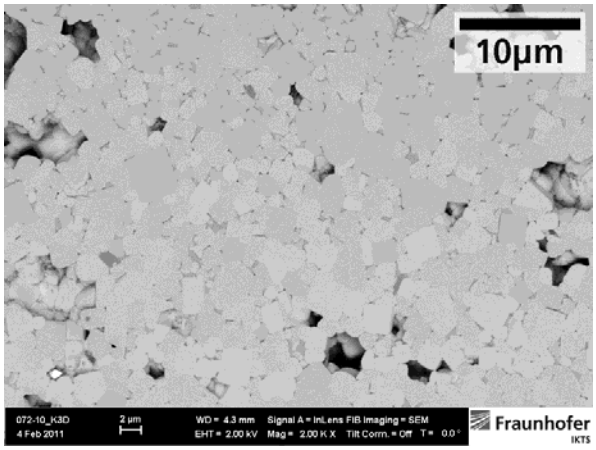

Fig. 2: Microstructure of the PZ 5100 thick film (cross section) with 2000 x magnification

B. Electrode design

Electrode designs for the two modes of excitation were completely different. Through-thickness polarised structures required flat and continuous electrodes (Fig. 3a). In-plane polarised structures needed IDEs (Fig. 3b). The IDE design complied with the guidelines defined by Beckert et al.[17] The electrode width (*w*) complied to equation (2) and the electrode distance (*d)* with equation (3).

$$w \geq 1.5 \times t_{PZT} \tag{2}$$

$$d \geq 4 \times t_{PZT} \tag{3}$$

The PZT thickness t_{PZT} was set to be 100 µm. Following equations (2) and (3) the electrode width *w* was defined to be 150 µm. Electrode distance *d* was fixed between 400 and 1000 µm with an increment of 200 µm. In literature, even thinner electrode widths of ~50 µm are recommended. Calculations by Beckert et al. showed that this will lead to field and stress intensity peaks at the electrode edges causing damage to the piezoceramic.[17] Furthermore, electrode width of 150 µm ensured an accurate and reproducible print layout over high topography.

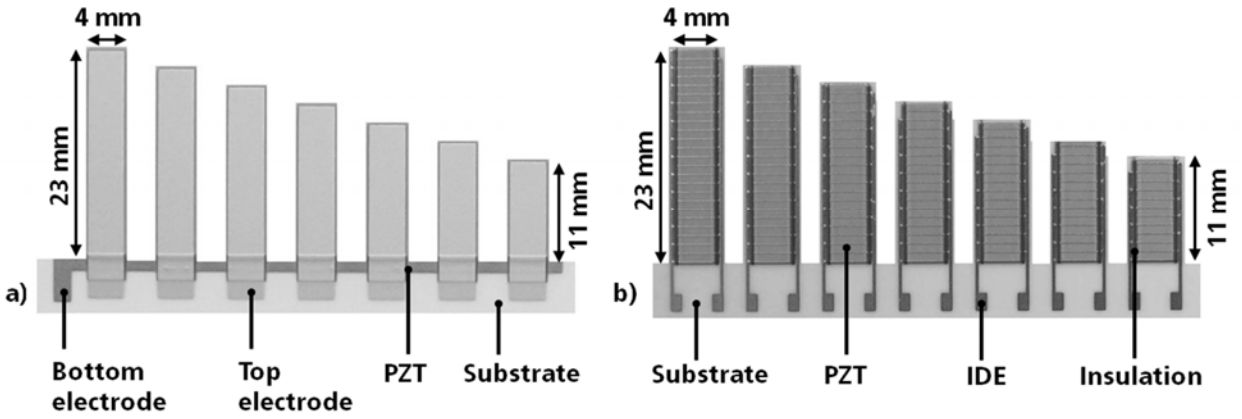

Fig. 3: Cantilever comb structures with a) flat continuous electrodes and b) interdigitated electrodes

C. Small and large signal properties

The samples were poled in air and at room temperature for 2 minutes with a nominal E-field E = 2 kV mm^{-1}, defined by the electrode distance. These poling conditions are sufficient for poling the soft PZT material. The capacity C and the dielectric loss factor tan δ were measured 24 h after poling at U_{AC} = 1 V and f =1 kHz using an impedance analyser (Hewlett Packard HP 4191A). Relative permittivity $\varepsilon^{T}_{33}/\varepsilon_0$ was calculated using equation (4) where A is the active area.

$$\varepsilon_{33}^{T} = \frac{Ct_{PZT}}{\varepsilon_0 A} \tag{4}$$

Free displacements and blocking forces were characterised for different cantilever lengths and various electrode configurations (see below). For each cantilever length, at least 4 samples were measured.

- through-thickness
- IDE 400 µm electrode distance
- IDE 600 µm electrode distance
- IDE 800 µm electrode distance
- IDE 1000 µm electrode distance

Attaching cantilever comb structures to aluminium blocks with epoxy (Araldite® 2020, Huntsman) facilitated mounting into the sample holder in a vertical orientation. Hence, the cantilevers bent freely during excitation with an electrical field or E = 2 kV mm^{-1} which was chosen to gain a large performance and being safe from electrical break down. A laser triangulation sensor (LK-H022, Keyence) measured the free displacement at the cantilever's tip with a resolution of 0.25 µm. During force measurement a force sensor (KD78, ME-Messsysteme) inhibited the displacement and measured the blocking force of the cantilever. An x-y-positioning stage with an accuracy of ± 2 µm compensated for the design-related elasticity of the force sensor.

D. FEM-Simulations

In the experiment, performance dependence on the IDE distance was expected on account of inactive regions beneath the electrodes. To achieve a deeper understanding of the behaviour of in-plane polarised PZT thick film cantilever structures, 2D finite element simulations of electrode distance dependences were carried out

using ANSYS. The data set used for the calculations is depicted in Table 1. The elastic stiffness constants c_{ij}^{E} were assumed from bulk material data provided by the powder manufacturer[18]. The piezoelectric constants e were determined by fitting numerical calculations of characteristic bending curves to measured characteristic bending curves of through-thickness polarised cantilevers with PZ 5100 thick film on alumina as shown in Fig. 3a. The values of relative permittivity ε_r^S were determined experimentally on PZ 5100 thick film structures. The piezoelectric behaviour was assumed to be linear. The mesh-size of the calculations was at least 1/10 the element thickness *t*.

Table 1: Data set used for the simulations of PZT thick films (PZ 5100)

Elastic stiffness constant, c_{ij}^{E} / Nm^{-2}	$1\cdot10^{10}\cdot\begin{pmatrix} 12.71 & 7.86 & 7.87 & & & \\ 7.86 & 12.71 & 7.87 & & & \\ 7.87 & 7.87 & 11.1 & & & \\ & & & 2.92 & & \\ & & & & 2.92 & \\ & & & & & 2.42 \end{pmatrix}$
Piezoelectric constant, e / Cm^{-2}	$\begin{pmatrix} & & & & 11.316 & 0 \\ & & & 11.316 & & \\ -1.704 & -1.704 & 15.99 & & & \end{pmatrix}$
Relative permittivity, ε_r^S	$\begin{pmatrix} 1320 & & \\ & 1320 & \\ & & 1475 \end{pmatrix}$

The E-field distribution was calculated for a homogeneous, horizontally poled piezo material with IDEs. The electric potential difference between opposing electrodes was set for a nominal electric field of E = 2 kV mm^{-1}. The electrode distance in a first simulation step varied between d = 200 and 3000 µm with an electrode width of w = 150 µm and a PZT thickness of t = 100 µm. In a second set of calculations, the PZT thickness varied between t = 10 and 200 µm with a constant electrode distance of d = 900 µm.

V. Results

A. Small and large signal properties

Relative permittivity of the PZ 5100 thick film was determined $\varepsilon^T_{33}/\varepsilon_0$ = 2100 and dielectric loss factor was measured tan δ = 0.04.

The measured data of free displacement and blocking force for both modes of excitation are summarised in Fig. 4. Each bar of the diagram represents a number of at least 4 samples. The two bending directions resulting from equation (1) were achieved in the experiments by the respective excitation mode. Using the through-thickness mode of excitation a cantilever of 23 mm length reached 89 µm free displacement and 74 mN blocking force. A cantilever of the same dimension using in-plane excitation generated free displacements between 125 µm and 147 µm and blocking forces between 130 mN and 150 mN depending on

the particular electrode distance. Compared to through-thickness excited cantilevers the in-plane excited cantilevers nearly doubled the values of free displacement and blocking force. This effect was expected from equation (1) but the improvement depended on the IDE design parameters. Smaller electrode distances led to smaller deflections. This can be explained by the electrical field distribution and the active length of PZT as discussed later.

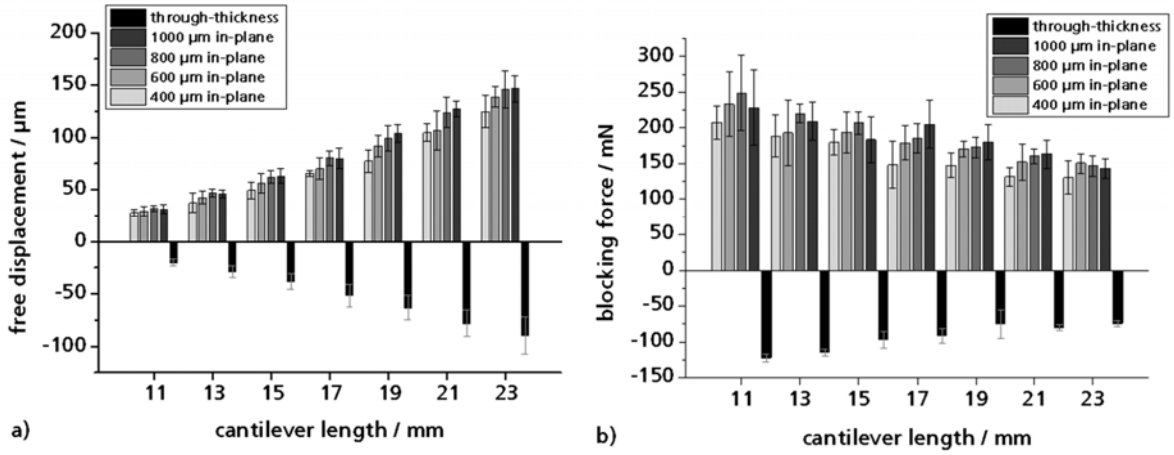

Fig. 4: a) Free displacement and b) blocking force of in-plane and through-thickness polarized cantilever

FEM Simulations by Hufenbach et al. demonstrated that a lateral mismatch of electrode fingers of bottom and top electrode is relevant to E-field distribution when using IDEs.[19] The permissible mismatch is defined to ± 0.05 mm. Larger mismatches lead to more diagonal field lines. Consequently, such an actuator would behave more like a through-thickness mode cantilever. However, the positioning accuracy of the screen-printing technology is below 50 µm. Therefore, the influence should be within this range.

B. FEM-Simulations

To explain performance dependence on the electrode distance, 2-dimensional finite element simulations of the electrical field distribution of the PZT are conducted. The length of a cantilever segment l_T reached from the centre of one electrode to the centre of the next one. Symmetry was used to restrict the simulation to the half-space from centre of one electrode to the centre of the segment. The PZT material was assumed to behave linear and to be homogeneously polarised along the x-axis. Voltage boundary conditions were shown in Fig. 5a.

To reach a nominal electric field strength of E_{nom} = 2 kV mm^{-1} over the distance between electrodes potential in the plane of symmetry was set to U = 0 V and voltage at the centre of the electrode to the corresponding value according to equation (5) (here U = – 600 V).

$$U = E_{nom} \times \frac{d}{2} \tag{5}$$

The calculated field distribution is depicted in Fig. 5a. The field distribution between the electrodes was inhomogeneously as known from literature.[17] It reached beneath the electrodes and formed intensity peaks at their edges. At a distance from the electrodes that corresponded approximately to the PZT thickness the field was homogeneously, but did not reach the nominal field strength of 2 kV mm^{-1}.

A planar model was developed that defined a theoretical electrode distance d_{th} (Fig. 5b) from the voltage applied to the model and the field strength reached in the homogeneous region. This planar electrode distance in turn defined the active length of the PZT segment l_A as compared to the total length of the segment l_T.

A variation of the PZT thickness in the simulations found a dependence of the active length l_A on both the PZT thickness t_{PZT} and the electrode distance d given by equation (6) where $\Delta d = t_{PZT} \times 61 \pm 2\%$ (Fig. 6a).

$$l_A = d + \Delta d \tag{6}$$

This applied for electrode distances greater than 2 × t_{PZT}. The planar model now made it possible to drastically reduce the complexity in 3D simulations of large actuator layouts that incorporate IDE structures. The effective field strength was a function of the aspect ratio d/t_{PZT} of the segment and was calculated for different aspect ratios (Fig. 6b). It approached 2 kV mm^{-1} asymptotically for greater aspect ratios (greater electrode distances).

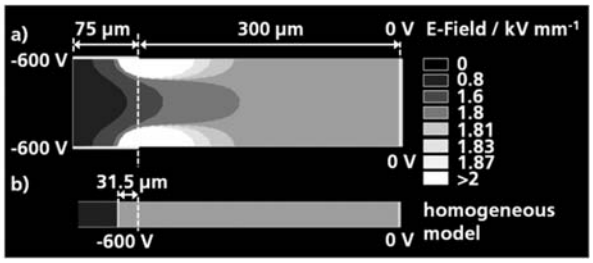

Fig. 5: a) E-field distribution on an in-plane polarized PZT thick film; b) homogeneous model

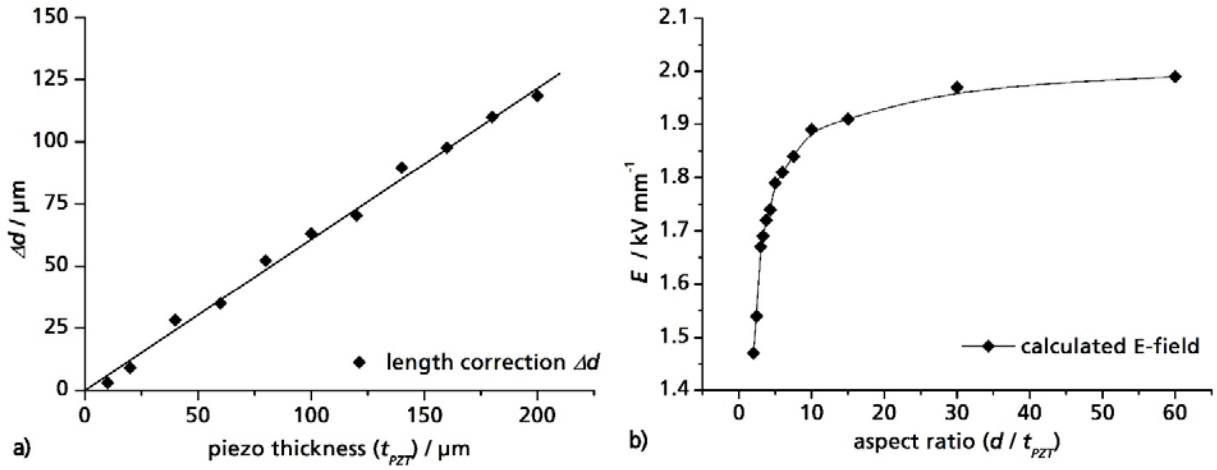

Fig. 6: a) Length correction Δd based on the piezo thickness t_{PZT}, b) E-field in the homogeneous region between two electrodes as function of the aspect ratio (d/t_{PZT})

In summary, the calculations resulted in an effective field strength, as compared to the nominal field strength and an active length, as compared to the segment length, dependent on the design parameters of the IDE structure (t_{PZT}, l_T, d). To compare the performance of different IDE designs a quality factor Q was defined as $Q = Q_A \times Q_E$, where Q_A is the ratio of the active length versus the total length of the segment in the planar model (l_A/l_T) and Q_E is the ratio of the effective versus the nominal field (E_{eff}/E_{nom}). The calculated values for

the designs fabricated in our experiments are summarised in Table 2. Q rised with increasing electrode distance. The geometric efficiency resulting from Q explained the dependences on the IDE distance found in the experiments. Dividing the measured data by the corresponding value for Q compensated the differences in performance. This is shown exemplarily in Fig. 7 where the measured data of free displacement of a 23 mm long cantilever were almost equalised when dividing them by Q.

Table 2: Calculated quality factors

d / µm	l_A / µm	l_T / µm	Q_A /%	E_{eff} / kV mm^{-1}	Q_E /%	Q /%
400	463	550	84.2	1.72	86.0	**72.4**
600	663	750	88.4	1.81	90.5	**80.0**
800	863	950	90.8	1.86	93.0	**84.4**
1000	1063	1150	92.4	1.88	94.0	**86.9**

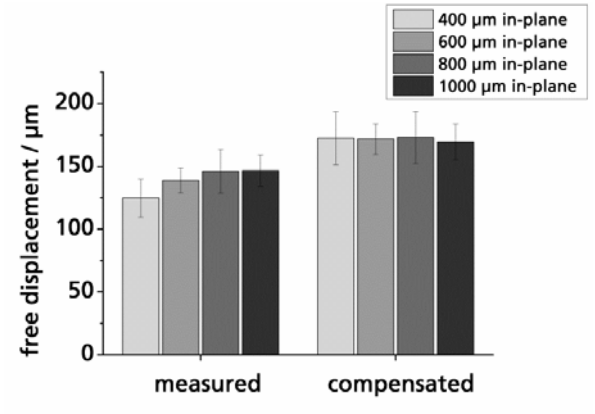

Fig. 7: Free displacement of 23 mm long cantilevers; measured data (left); data compensated for geometric efficiency (right)

Overall, both actuator types have assets and drawbacks. Through-thickness mode structures only require voltages between U = 60-300 V depending on piezoceramic film thickness to generate an electrical field of E = 2 kV mm^{-1}. A continuous electrode can act as a diffusion barrier and prevent chemical interactions with silicon containing substrates. Therefore, the variety of possible substrates is larger. The continuous electrode has a good adhesion to the substrate and the PZT thick film.

The IDE-type actuator performance is approximately twice the through-thickness polarised actuator performance when applying an E-field of E = 2 kV mm^{-1}. IDE structures need high voltages up to U = 2000 V depending on the electrode distance to reach this field strength. That, however, does not constitute a problem since miniaturised transformers are readily available. For IDEs precious metal consumption is very low which is a cost factor especially when using gold. However, depending on the requirements each actuator type has its advantages and it could be beneficial achieving both bending directions by a single-side coating process.

VI. Conclusions

In-plane polarised PZT thick film actuators were successfully fabricated with interdigitated electrodes. They showed excellent free displacements and blocking forces. The performance increased with rising electrode distance. From FEM simulations of the electrical field distribution the geometric efficiency Q was derived

that characterised the design dependent efficiency of IDE structures. A planarised model allowed for efficient simulation of complex actuator structures. The effective electrical field in the actuators was lower than the nominal field, but over a correspondingly longer active length, that reached beneath the electrodes. The larger the electrode distance, the lower the impact of inactive regions on the actuator performance. The in-plane mode of excitation improved the actuator stroke by a factor ~2 compared to the through-thickness mode.

VII. Acknowledgement

The authors gratefully acknowledge the support by our co-workers Matthias Reitz and Susanne Schröder and the funding by the German Research Foundation (DFG) within the Priority Program Active Micro-optics.

The present paper is based on a proceedings paper of the Electroceramics for End-Users VII conference, PIEZO 2013, in France.

References

[1] S. E. Gebhardt, T. Rödig, U. Partsch and A. J. Schönecker: 'Development of Micro-integrated sensors and actuators based on PZT thik films', Proc. of the 16th Eur. Microelectron. and Packaging Conf. & Exhibition EMPC, **2007**, Vol. 2007

[2] S. Gebhardt, D. Ernst, B. Bramlage, M. Flössel, and A. Schönecker: 'Integrated Piezoelectrics for smart Microsystems-A Teamwork of Substrate and Piezo', Adv. in Sci. and Technol., 2013, **77**, 1-10

[3] Y. Qiu, H. Wang, A. Bolhovitins, C. Démoré, S. Cochran, S. Gebhardt, and A. Schönecker: 'Thick Film PZT Transducer Arrays for Particle Manipulation', Proc. of 2013 Joint UFFC, EFTF and PFM Symp., Prague, Czech Republic, 21-25 July, **2013**, 1911-1914, ISBN 978-1-4673-5686-2

[4] D. Zhu, P. Glenne-Jones, N. White, N. Harris, J. tudor, R. Torah, A. Almusallam and S. Beeby: 'Screen printed piezoelectric films for energy harvesting', Advances in Applied Ceramics, 2013, **112**, (2), 79-84, http://dx.doi.org/10.1179/1743676112Y.0000000022

[5] C. G. Hindrichsen, R. Lou-Møller, K. Hansen, E.V. Thomsen: 'Advantages of PZT thick film for MEMS sensors', Sensors and Actuators A: Phys., 2010, **163**, (1), 9-14, ISSN 0924-4247, http://dx.doi.org/10.1016/j.sna.2010.05.004

[6] M. Kosec, D. Kuscer, J. Holc: 'Processing of Ferroelectric Ceramic Thick Films', in 'Multifunctional Polycrystalline Ferroelectric Materials', Springer Netherlands, **2001**, 39–61, doi:10.1007/978-90-481-2875-4_2

[7] J. H. Park, H. Kim, D. S. Yoon, S. Y. Kwang, J. H. Lee, T. S. Kim: 'Effects of the material properties on piezoelectric PZT thick film micro cantilevers as sensors and self actuators', J. of Electroceram.,2010, **25**, (1), 1–10, doi:10.1007/s10832-009-9581-z

[8] R. Lakhmi, H. Debeda, M. Maglione, I. Dufour, C. Lucat: 'Study of Screen-Printed PZT Cantilevers Both Self-Actuated and Self-Read-Out', Int. J. of Appl. Cer. Technol., **2013**, http://dx.doi.org/10.1111/ijac.12006

[9] A. A. Bent: 'Active Fiber Composites for Structural Actuation', Doctor of philosophy Dissertation, Massachusetts Institute of Technology, USA, January 1997

[10] W. K. Wilkie, R. G. Bryant, J. W. High, R. L. Fox, R. F. Hellbaum, A. Jalink Jr., B. D. Little and P. H. Mirick: 'Low-cost piezocomposite actuator for structural control applications', Proc. SPIE 3991, Smart Structures and Mater. 2000: Ind. and Commercial Applications of Smart Structures Technol., 2000, **323** , doi:10.1117/12.388175

[11] B. Xu, L. Eric Cross and J. J. Bernstein: 'Ferroelectric and Antiferroelectric Films for Microelectromechanical Systems Applications', Thin Solid Films, 2000, **377** , 712-718

[12] N. M. White, V. T. K. KO: 'Thick-film acoustic wave sensor structure', Electron. Letters, 1993, **29**, (20), 1807-1809, doi: 10.1049/el:19931202

[13] G. De Cicco and B.Morten: 'Thick-film Piezoelectric Actuators for Micropositioning', J. of Intelligent Mater. Systems and Structures, 2009, **20**, (14), 1689-1697, doi: 10.1177/1045389X09341201

[14] R. N. Torah, S. P. Beeby, M. J. Tudor and N. M. White: 'Thick-film Piezoceramics and devices', J. of Electroceram. 2007,**19**, (1), 97-112

[15] Ceram Tec GmbH, „Special materials Sonox® P51", datasheet

[16] D. Ernst, B. Bramlage, S. Gebhardt, A. Schönecker, O. Pabst, and H.-J. Schreiner: 'Enhanced Large Signal Performance of PZT Thick Film Actuators for Active Micro-Optics', Proc. of 2013 Joint UFFC, EFTF and PFM Symp., Prague, Czech Republic, 21-25 July, **2013**, 5-8, ISBN 978-1-4673-5996-2

[17] W. Beckert, W. S. Kreher: 'Modelling piezoelectric modules with interdigitated electrode structures', Computational Mater. Sci., 2003, **26**, 36-45, http://dx.doi.org/10.1016/S0927-0256(02)00390-7

[18] H.J. Schreiner, Ceram Tec GmbH, personal communication

[19] W. Hufenbach, M. Gude and T. Heber: 'Design and testing of novel piezoceramic modules for adaptive thermoplastic composite structures', Smart Mater. and Structures, 2009, **18**, (4), 045012, doi: 10.1088/0964-1726/18/4/045012